TECHNICAL UNIVERSITY OF CLUJ-NAPOCA

ACTA TECHNICA NAPOCENSIS

Series: Applied Mathematics, Mechanics, and Engineering
Vol. 66, Issue II, June, 2023

EXPERIMANTAL VALIDATION OF THE NEW THEORETICAL MODEL OF INTERFERENCE FITS

Simion HARAGÂŞ, Ovidiu BUIGA, Lucian TUDOSE

Abstract: *Bearings are, in general, mounted with an interference fit on the shaft or in the housing. During the pressing phase, expansion/compression of the bearing rings and the mating assembly parts occur, influencing the operating bearing clearance. This paper refers to a new theoretical model which was developed for the exact calculation of the dimensionless coefficient -* K_{ie} *and also for the radial displacements (suffered by the hub and shaft during the pressing phase) used in the case of an interference-fitted fastener to achieve the desired operational clearance. To validate the new mathematical model an experimental analysis of the interference-fit was carried out. In this vein, two sets of experimental specimens were produced. The first set has the shaft and the hub made of quenched and tempered - 41CrMo4 alloy steel and C45 respectively; for the 2nd set, the shaft is made of C45 and the hub is from X6CrNiTi18-10. It could be observed that the results from the two approaches i.e. theoretical and experimental were consistent and in relatively good agreement.*

Key words: *interference fit connection, operational internal clearance, contacting pressure, radial displacements.*

1. INTRODUCTION

In mechanical engineering applications, when is a need for rotational or torque transmission between the shaft and the gear, pulleys, chain wheels etc. mounted on it, shaft-hub-connections should be used. From this category interference-fitted connection is widely accepted for achieving these purposes. The nature [1] of this joint consists of selecting the hub diameter bore's i.e. the bushing smaller than the shaft. Interference fit assembly is widespread among hub-shaft connections considering their advantages, such as being compact, rigid, effective [2], and due to the ease of mechanical processing (of the assembly elements). When assembling shafts and hubs using interference fitted joints aspects regarding stress concentration (due to the contacting surfaces of the assembly) and fretting fatigue phenomenon (characterized by a very small oscillatory amplitude (less than 100 µm) [3] which conduct to a large deterioration and wear with a significant decrease of mechanical components fatigue life) occurs [2]. The connection fitted fatigue life is improved up to 50% [2] by selecting the proper configuration (various values of the fillet, different shapes, and dimensions of the groove, or an overhung hub). Juuma in [4], respectively Nishioka and Komatsu [5] demonstrate this through several experimental tests. Regarding the fretting phenomenon at this moment, in the technical literature, there are important studies that deal with this issue applied to interference fits. For example, in [6] two modeling techniques were used for analyzing the failure of the gear hub/shrink-fit assembly. The authors of this research concluded that the slip and the corresponding fretting occur due to another failure mechanism leading to an increase in the gear hub diameter. There are some studies such as [7], [8], or [11] in which there is used finite element analysis for modeling this phenomenon. In [7] is analyzed the propagation and development of a crack in a shrink-fit assembly. Here were used two finite element models were to assess the fretting load and to determine the

Received: 13.03.23; **Similaritie**s: 29.05.23: **Reviewed**: 31.05./26.05.23: **Accepted**:20.06.23.

growth of the crack. In [8], a finite element analysis (FEA) based on Smith-Watson-Topper (SWT) [9] fatigue parameter considering multiaxial aspects for spline design is presented. The implementation is compared with the experimental and theoretical results presented in [10]. In [11] six different shrink-fit forms are modeled and analyzed by the means of the FEA methodology which gives more accurate results than the traditional ones. An interesting analogy between experimental trials and FEA for various configurations of interference fits in rotating bending and alternated torsion is presented in [12]. Here von Mises, Sine, Crossland and Dang Van criteria were used to assess the fatigue results. Hattori et al. in [13] describe estimation methods to determine the fretting wear process and fretting fatigue life. Li et al in [14] present experimental investigations carried out on reinforced polymer CFRP/Ti alloy bolted joints (widespread in a structure such as movable wing, fuselage etc.). They determine the dependencies between the interference fit sizes and the fretting fatigue life for different stress levels.

In this paper, an effort was carried out to develop a new theoretical model for the exact computation of the dimensionless coefficient K_{ie} and the radial displacements (suffered by the hub and shaft during the pressing operation) used in the case of interference-fitted fastener (section 2) to achieve the desired operational clearance. Then, the new mathematical model is validated through experimental tests (section 3). Eventually, the discussion is concluded with some reflections and suggestions regarding the possible extensions of the present study.

2.NEW METHODOLOGY FOR INTERFERENCE FIT CALCULATION

This section describes the new theoretical approach developed for the complete calculus of a heated-fitted interference connection. Let now us consider two different heated ($t_i(r)$; $\phi_i \leq r \leq \phi$ and $t_e(r)$; $\phi \leq r \leq \phi_e$, respectively) hollow cylinders (index i, for the inner cylinder - fig.1a; and index e for the outer cylinder – fig.1a) of different material (E_i, ν_i, α_i and E_e, ν_e, α_e, respectively) that are tight fitted together (fig. 1b). Both cylinders are free to expand axially. In the following, the value of the effective interference is denoted by I (calculated as ϕ_1 - ϕ_2). This assembly can be made either by pressing the inner cylinder into the hole of the outer cylinder or by heating (cooling) the outer (inner) cylinder, bringing the cylinders into the desired position, and waiting until the fitting is achieved. After all these, the cylinders are subjected to a different distribution of temperatures.

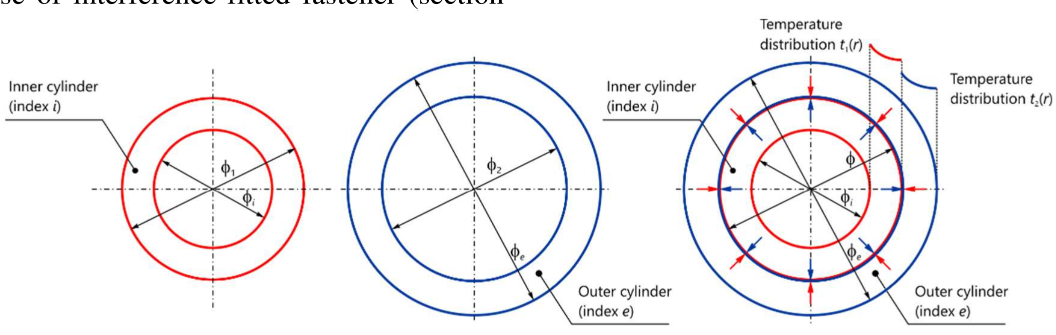

Fig.1 Interference-fitted connection of two heated hollow cylinders
a) the two parts (shaft - inner cylinder and hub - outer cylinder, respectively) before the assembly;
b) the fitted-assembly.

During the assembling, the inner cylinder is compressed, and the outer cylinder is expanded. After stabilizing the assembly, the matching diameter of the two cylinders reaches some value denoted here by ϕ. This value, according to classical approaches [15] is assumed to be the nominal value of the diameters of the shrink parts. Considering the principle under which, within any natural phenomenon only the strictly necessary energy will be spent to obtain the desired outcome, the stabilization of the assembly will be made at such a diameter ϕ that the amount of total work spent is minimal [16]. From [16] the exact value of the equilibrium matching diameter ϕ of the tight fit is given by:

$$\phi = \phi_1 - \frac{1}{1+K_{ie}} \cdot I_{ie} \qquad (1)$$

where: I_{ie} is the interference-fit, computed as:

$$I_{ie} = \phi_1 - \phi_2 \qquad (2)$$

and the "factor of interference" [16], [17] is:

$$K_{ie} = \frac{E_i}{E_e} \cdot \frac{1+\nu_1}{1+\nu_2} \cdot \frac{\phi_1^2 - \phi_i^2}{\phi_e^2 - \phi_2^2} \cdot \frac{\phi_i^2 + (1-2\cdot\nu_1)\cdot\phi_1^2}{\phi_e^2 + (1-2\cdot\nu_2)\cdot\phi_2^2} \cdot \left[\frac{(1+\nu_2)\cdot\phi_e^2 + (1-\nu_2)\cdot\phi_2^2}{(1+\nu_1)\cdot\phi_i^2 + (1-\nu_1)\cdot\phi_1^2}\right]^2 \qquad (3)$$

At the level of the interface fit of the two bodies, a certain contact pressure p is developed. After the different heating of the two cylinders, this pressure will change magnitude. A loos fi is also possible. In the following stress and displacement denotation, a certain rule of indexes was established: **1.** the first index assigned to the stress - σ_r and the displacement - u classic symbols (used in technical literature) show the body to which the respective stress or displacement refers; **2.** the following indexes indicate the diameter to which the respective stress or displacement are referring.

The equation of the contacting pressure is:

$$p = \max\left(0, \frac{1}{K_{ie}} \cdot \left[\frac{I_{ie}}{\phi} + \alpha_i \cdot \frac{8}{\phi^2 - \phi_i^2} \cdot \int_{\phi_i/2}^{\phi/2} r \cdot t_i \cdot \mathrm{d}r - \alpha_e \frac{8}{\phi_e^2 - \phi^2} \cdot \int_{\phi/2}^{\phi_e/2} r \cdot t_e \cdot \mathrm{d}r\right]\right) \qquad (4)$$

Once the contacting pressure is computed, all values of stresses and displacements can be obtained as follows:

The radial stresses are:

$$\sigma_{r i \phi} = \sigma_{r e \phi} = -p \ , \ \sigma_{r i \phi i} = \sigma_{r e \phi e} = 0 \qquad (5)$$

The circumferential stresses:

$$\sigma_{\theta i \phi i} = -\frac{2\cdot\phi^2}{\phi^2 - \phi_i^2} \cdot p + \alpha_i \cdot \frac{E_i}{1-\nu_i} \cdot \left[\frac{8}{\phi^2 - \phi_i^2} \cdot \int_{\phi_i/2}^{\phi/2} r \cdot t_i \cdot \mathrm{d}r - t_i \cdot \left(\frac{\phi_i}{2}\right)\right] \qquad (6)$$

$$\sigma_{\theta i \phi} = -\frac{\phi^2 + \phi_i^2}{\phi^2 - \phi_i^2} \cdot p + \alpha_i \cdot \frac{E_i}{1-\nu_i} \cdot \left[\frac{8}{\phi^2 - \phi_i^2} \cdot \int_{\phi_i/2}^{\phi/2} r \cdot t_i \cdot \mathrm{d}r - t_i \cdot \left(\frac{\phi}{2}\right)\right] \qquad (7)$$

$$\sigma_{\theta e \phi} = -\frac{\phi_e^2 + \phi^2}{\phi_e^2 - \phi^2} \cdot p + \alpha_e \cdot \frac{E_e}{1-\nu_e} \cdot \left[\frac{8}{\phi_e^2 - \phi^2} \cdot \int_{\phi/2}^{\phi_e/2} r \cdot t_e \cdot \mathrm{d}r - t_e \cdot \left(\frac{\phi}{2}\right)\right] \qquad (8)$$

$$\sigma_{\theta e \phi e} = \frac{2\cdot\phi^2}{\phi_e^2 - \phi^2} \cdot p + \alpha_e \cdot \frac{E_e}{1-\nu_e} \cdot \left[\frac{8}{\phi_e^2 - \phi^2} \cdot \int_{\phi/2}^{\phi_e/2} r \cdot t_e \cdot \mathrm{d}r - t_e \cdot \left(\frac{\phi_e}{2}\right)\right] \qquad (9)$$

where: $E_{i,e}$ - are the modulus of elasticity in tension and compression (Young's modulus) for shaft and hub material, in MPa; $\nu_{i,e}$ - are the Poisson's ratio. The axial stresses:

$$\sigma_{z i \phi i} = \alpha_i \cdot \frac{E_i}{1-\nu_i} \cdot \left[\frac{8}{\phi^2 - \phi_i^2} \cdot \int_{\phi_i/2}^{\phi/2} r \cdot t_i \cdot \mathrm{d}r - t_i \cdot \left(\frac{\phi_i}{2}\right)\right] \qquad (10)$$

$$\sigma_{zi\phi} = \alpha_i \cdot \frac{E_i}{1-\nu_i} \cdot \left[\frac{8}{\phi^2 - \phi_i^2} \cdot \int_{\phi_i/2}^{\phi/2} r \cdot t_i \cdot \mathrm{dr} - t_i \cdot \left(\frac{\phi}{2} \right) \right] \tag{11}$$

$$\sigma_{ze\phi} = \alpha_e \cdot \frac{E_e}{1-\nu_e} \cdot \left[\frac{8}{\phi_e^2 - \phi^2} \cdot \int_{\phi/2}^{\phi_e/2} r \cdot t_e \cdot \mathrm{dr} - t_e \cdot \left(\frac{\phi}{2} \right) \right] \tag{12}$$

$$\sigma_{ze\phi e} = \alpha_e \cdot \frac{E_e}{1-\nu_e} \cdot \left[\frac{8}{\phi_e^2 - \phi^2} \cdot \int_{\phi/2}^{\phi_e/2} r \cdot t_e \cdot \mathrm{dr} - t_e \cdot \left(\frac{\phi_e}{2} \right) \right] \tag{13}$$

The radial displacements are:

$$u_{i\phi i} = \frac{\phi_i}{2} \cdot \left(-\frac{1}{E_i} \cdot \frac{2 \cdot \phi^2}{\phi^2 - \phi_i^2} \cdot p + \alpha_i \cdot \frac{8}{\phi^2 - \phi_i^2} \cdot \int_{\phi_i/2}^{\phi/2} r \cdot t_i \cdot \mathrm{dr} \right) \tag{14}$$

$$u_{i\phi} = \frac{\phi}{2} \cdot \left[-\frac{1}{E_i} \cdot \frac{(1-\nu_i) \cdot \phi^2 + (1+\nu_i) \cdot \phi_i^2}{\phi^2 - \phi_i^2} \cdot p + \alpha_i \cdot \frac{8}{\phi^2 - \phi_i^2} \cdot \int_{\phi_i/2}^{\phi/2} r \cdot t_i \cdot \mathrm{dr} \right] \tag{15}$$

$$u_{e\phi} = \frac{\phi}{2} \cdot \left[\frac{1}{E_e} \cdot \frac{(1+\nu_e) \cdot \phi_e^2 + (1-\nu_e) \cdot \phi^2}{\phi_e^2 - \phi^2} \cdot p + \alpha_e \cdot \frac{8}{\phi_e^2 - \phi^2} \cdot \int_{\phi/2}^{\phi_e/2} r \cdot t_e \cdot \mathrm{dr} \right] \tag{16}$$

$$u_{e\phi e} = \frac{\phi_e}{2} \cdot \left[\frac{1}{E_e} \cdot \frac{2 \cdot \phi^2}{\phi_e^2 - \phi^2} \cdot p + \alpha_e \cdot \frac{8}{\phi_e^2 - \phi^2} \cdot \int_{\phi/2}^{\phi_e/2} r \cdot t_e \cdot \mathrm{dr} \right] \tag{17}$$

Considering a linear distribution of temperature between $T_i = t_i(\phi_i/2)$ (temperature of inner cylinder bore) and $T_e = t_e(\phi_e/2)$ (temperature of the outer cylinder surface) one obtains:

$$t_i(r) = t_e(r) = \frac{2 \cdot (T_e - T_i)}{\phi_e - \phi_i} \cdot r + \frac{\phi_e \cdot T_i - \phi_i \cdot T_e}{\phi_e - \phi_i} \tag{18}$$

$$a = \frac{2 \cdot (T_e - T_i)}{\phi_e - \phi_i}, \; b = \frac{\phi_e \cdot T_i - \phi_i \cdot T_e}{\phi_e - \phi_i} \tag{19}$$

In these conditions the important radial displacements are:

$$u_{i\phi i} = \frac{\phi_i}{2} \cdot \left[-\frac{1}{E_i} \cdot \frac{2 \cdot \phi^2}{\phi^2 - \phi_i^2} \cdot p + \alpha_i \cdot \left(\frac{a}{3} \cdot \frac{\phi^3 - \phi_i^3}{\phi^2 - \phi_i^2} + b \right) \right] \tag{20}$$

$$u_{e\phi e} = \frac{\phi_i}{2} \cdot \left[\frac{1}{E_i} \cdot \frac{2 \cdot \phi^2}{\phi_e^2 - \phi^2} \cdot p + \alpha_e \cdot \left(\frac{a}{3} \cdot \frac{\phi_e^3 - \phi^3}{\phi_e^2 - \phi^2} + b \right) \right] \tag{21}$$

3. EXPERIMENTAL TESTS AND VALIDATION

At this phase of experimental validation regarding the new mathematical model, the practical tests were carried out without considering the influence of the temperature over the press-fit. This aspect will be treated in further research. The experimental tests were performed taking into account two sets of interference-fitted connections. For the first set, the shaft and the hub are made of quenched and tempered - 41CrMo4 alloy steel and C45 respectively; for the 2^{nd} set, the shaft is made of C45 and the hub is from X6CrNiTi18-10. In table 1 are shown the mechanical characterization of the mechanical components i.e. shaft and hub, respectively.

Table 1

Materials mechanical characterization

Material - EN designation/material no.	**Young's modulus of elasticity E,** MPa	**Poisson's ratio, ν**
41CrMo4 / 1.7225	$(2…2.07) \cdot 10^5$	0.27…0.3
C45 / 1.0503	$2.02 \cdot 10^5$	0.27…0.3
X6CrNiTi18-10 / 1.4541	$2 \cdot 10^5$	0.3

Figure 2 presents the geometry of the interference-fitted fastener.

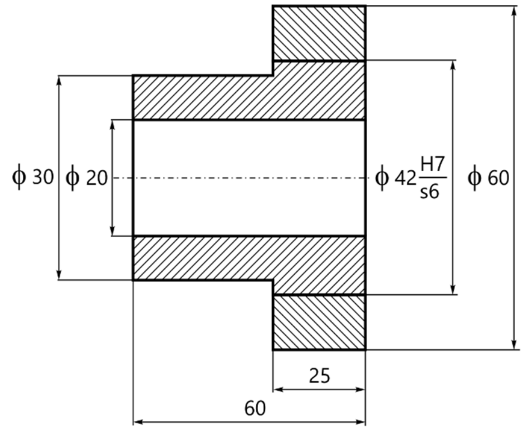

Fig.2 Geometry and dimensions of the interference-fitted connection

Once the hubs and the shafts have been mechanical processed (by grinding) their surface roughnesses are measured using a *TR*220 tester. For each investigated surface, the tester sensor is moved along the linear measured surface. These movements are converted into electric signals and then refined by the *PT*220 tester main processor as R_z values. In fig. 3 and 4 are highlighted the R_z values for hubs and shafts (for both sets of materials). In Table 2 (column 3) the values of R_z are shown (they are computed as the arithmetic mean of three measurements).

Fig. 3 Hub surface roughness measured with *TR*220 tester
a) the first set (**H-S1_01,02,03**); **b)** the second set (**H-S2_01,02,03**).

Fig. 4 Shaft surface roughness measured with TR220 tester
a) the first set (**S-S1_01,02,03**); **b)** the second set (**S-S2_01,02,03**);

In figure 5 are presented the measurements of the interference fit with the Werth measuring machine.

The measured values are compared (Table 2) with the corrected ones (computed with equation 1 of the mathematical model described in section 2). The calculated values of the equilibrium matching diameter ϕ are presented in the last column of the above table.

Fig. 5 Interference-fit measured with Werth machine

Table 2

Side-by-side comparison between interference-fitted connection measured and computed

Experimental specimens	**Material EN designation/material no.**	R_z, [μm]	**Shaft & hub dimensions before the assembly**				**Shaft & hub dimensions after the assembly**			
			ϕ_1, [mm]	ϕ_2, [mm]	ϕ_i, [mm]	ϕ_e, [mm]	ϕ_i, [mm]	ϕ_e, [mm]	**Interference-fitted dimension - measured ϕ_2/ϕ_1**	**Interference-fitted dimension - computed ϕ_2/ϕ_1**
Shaft*d*	41CrMo4 / 1.7225	2.855	42.054		19.96		19.895		**42.047**	**42.043**
Hub *D*	C45 / 1.0503	3.916		42.02		79.971		80.061		
Shaft *d*	C45 / 1.0503	2.778	42.058		20.15		20.115		**42.042**	**42.04**
Hub *D*	X6CrNiTi18-10 / 1.4541	3.123		42.008		79.972		79.999		

4. CONCLUSIONS

Bearings are mounted in most cases by pressing them on the shafts. During this process, important expansion/compression of the bearing inner/outer ring occurs influencing the operating bearing clearance. In this paper, a new theoretical model was developed for the exact calculation of the dimensionless coefficient - K_{ie} and also for the radial displacements used in the case of an interference-fitted fastener to achieve the desired operational clearance. Although the new mathematical model takes into account the effect of the temperature over the press-fit, at this stage of the experimental tests the influence of the temperature is not considered. To validate the mathematical model two sets of experimental specimens were manufactured. The first set has the shaft made of quenched and tempered - 41CrMo4 alloy steel and C45 respectively; for the 2nd set, the shaft is made of C45 and the hub is from X6CrNiTi18-10. After the mechanical processing of the fitted connection parts, their roughness surfaces were measured using a TR220 tester. Next, the parts are assembled (press-fitted), and using the Werth machine are measured the real interference for both specimens. It could be observed that the results from the two approaches theoretical and experimental were consistent and in relatively good agreement. In further experimental research, efforts will be made to take into account the effects of the temperature on the interference-fit fastener.

5. REFERENCES

[1] Grote, K.H., Antonsson, E.K. *Springer handbook of mechanical engineering*, Springer, 2009.

[2] Biron, G., Vadean, A., Tudose, L. *Optimal design of interference fit assemblies subjected to fatigue loads,* Structural and Multidisciplinary Optimization, 47 (3), pp. 441-451, 2012.

[3] Lanoue, F., Vadean, A., Sanschagrin, B. *Finite element analysis, and contact modeling considerations of interference fits for fretting fatigue strength calculations*, Simulation Modelling Practice and Theory, 17, 10, pp. 1587-1602, 2009.

[4] Juuma, T. *Torsional fretting fatigue strength of a shrink-fitted shaft with a grooved hub*, Tribology International, 33, 8.

[5] Nishioka, K., Komatsu, H. *Researches on increasing the fatigue strength of press-fitted shaft assembly*, Bull JSME 10, 42, pp. 880-889, 1967.

[6] Truman, C.E., Booker, J.D. *Analysis of a shrink-fit failure on a gear hub/shaft assembly*, Engineering Failure Analysis, 14, 4, 2007, pp. 557-572.

[7] Gutkin, R., Alfredsson, B. *Growth of fretting fatigue cracks in a shrink-fitted joint subjected to rotating bending*, Engineering Failure Analysis, 15, 5, pp. 582-596, 2008.

[8] Sum, W.S., Williams, E.J., Leen, S.B. *Finite element, critical-plane, fatigue life prediction of simple and complex contact configurations*, International Journal of Fatigue, 27, 4, pp. 403-416, 2005.
[9] Smith, K.N., Watson, P., Topper, T.H. *A stress-strain function for the fatigue of metals*, J Mater, 15, pp. 767-778, 1970.
[10] Araujo, J.A., Nowell, D. *The effect of rapidly varying contact stress fields on fretting fatigue*, Int J Fatigue, 24, pp. 763-775, 2002.
[11] Ozel, A., Temiz, S., Aydin, M.D., Sen, S. *Stress analysis of shrink-fitted joints for various fit forms via finite element method*, Materials and Design, 26, 4, pp. 281-289, 2005.
[12] Lanoue F., Vadean, A., SAnschagrin, B. *Fretting fatigue strength reduction factor for interference fits*, Simulation Modelling Practice and Theory, 19, pp. 1811–1823, 2011.
[13] Hattori, T., Watanabe, T. *Fretting fatigue strength estimation considering the fretting wear process*, Tribology International, 39, pp. 1100-1105, 2006.
[14] Li, J., Zhang, K., Li, Y., Liu, P., Xia, J. *Influence of interference-fit size on bearing fatigue response of single-lap carbon fiber reinforced polymer/Ti alloy bolted joints*, Tribology International, 93, Part A, pp. 151-162, 2016.
[15] Harris, T.A., Kotzalas, M.N. *Essential Concepts of Bearing Technology* (*Rolling Bearing Analysis, Fifth Edition*), Taylor and Francis, 2007.
[16] Tudose, L., Kulcsar, G., Stănescu, C. *Influence of mounting tolerances and temperature on stresses and radial expansion of bearing rings*, RKB Bearing Industries Technical Review, 2011.
[17] Tudose, L., Kulcsar, G., Stanescu, C. *Influences of mounting tolerances and operating temperature on stresses and radial expansions of bearing rings*, RKB Bearing Industries Internal Technical Report, 2013.

Validarea experimentală a noului model teoretic al ajustajelor cu strângere

Rezumat: Rulmenții sunt, în general, montați cu strângere pe arbore sau în carcasă. În timpul fazei de presare, are loc o dilatare/comprimare a inelelor rulmentului și a pieselor de asamblare corespunzătoare, influențând jocul în funcționare al rulmentului. Această lucrare se referă la un nou model teoretic care a fost dezvoltat pentru calculul exact al coeficientului adimensional - K_{ie} și, de asemenea, pentru deplasările radiale (suferite de butuc și arbore în timpul fazei de presare) utilizate în cazul unei montări cu ajustaj cu strângere pentru a obține jocul de funcționare dorit. Pentru a valida noul model matematic a fost efectuată o analiză experimentală a asamblării cu strângere. În acest sens, au fost realizate două seturi de epruvete experimentale. Primul set are arborele și butucul realizate din oțel aliat 41CrMo4 și, respectiv, C45 călit și revenit; pentru cel de-al doilea set, arborele este realizat din C45, iar butucul este din X6CrNiTi18-10. S-a putut observa că rezultatele obținute prin cele două abordări, și anume teoretică și experimentală, au fost consecvente și în concordanță relativ bună.

Simion HARAGÂŞ, Professor Ph.D. Eng., Technical University of Cluj-Napoca, Mechanical Engineering Department, Romania, e-mail: Simion.Haragas@omt.utcluj.ro
Ovidiu BUIGA, Ass. Professor Ph.D. Eng., Technical University of Cluj-Napoca, Mechanical Engineering Department, Romania, e-mail: Ovidiu.Buiga@omt.utcluj.ro
Lucian TUDOSE, Professor Ph.D. Eng., Technical University of Cluj-Napoca, Mechanical Engineering Department, Romania, e-mail: Lucian.Tudose@omt.utcluj.ro